

Analysing High-Dimensional Neuroscience Models: Neurovascular Coupling.

Tim David¹, Pierre Gremaud², Joey Hart²

1.Department of Mechanical Engineering,

University of Canterbury, New Zealand

2.Department of Mathematics,

North Carolina State University, Raleigh, NC

July 30, 2018

Abstract

abstract here

1 INTRODUCTION

During the last two decades functional magnetic resonance imaging (fMRI) has proven to be an established tool in studying the human brain. This is especially true in the case of the blood-oxygen-level dependent (BOLD) signal, where changes in blood oxygen levels can

be detected via the magnetic signal [17]. However due to the constraint on the resolution of BOLD, fMRI methodology has not been used extensively to study the underlying cellular neural architecture and their associated cerebral functions. Complex models that address this important relationship and constructing a detailed compartmental model with the relevant cell types involved will allow simulations relating certain brain functions performed in a region to its fMRI BOLD response. The neurovascular coupling (NVC) mechanism, the cerebral metabolic rate of oxygen consumption, and the cerebral blood volume (CBV) are known to contribute to the fMRI BOLD response [3], however a thorough understanding of these factors has yet to be fully established.

The NVC response, the ability to locally adjust vascular resistance as a function of neuronal activity, is believed to be mediated by a number of different signalling mechanisms. Roy and Sherrington [19] first proposed a mechanism based on a metabolic negative feedback theory. According to this theory, neural activity leads to a drop in oxygen or glucose levels and increases in CO_2 , adenosine, and lactate levels. All of these signals could dilate arterioles and hence were believed to be part of the neurovascular response. However, recent experiments illustrated that the NVC response is partially independent of these metabolic signals [10, 11, 16, 18, 13]. An alternative to this theory was proposed where the neuron releases signalling molecules to directly or indirectly affect the blood flow. Many mechanisms such as the potassium (K^+) signalling mechanism [8], the nitric oxide (NO) signalling mechanism or the arachidonic acid to epoxyeicosatrienoic acid (EET) pathway are found to contribute to the neurovascular response [2].

The K^+ signalling mechanism of NVC seems to be supported by significant evidence, although new evidence shows that the endfoot astrocytic calcium (Ca^{2+}) could play a significant role. The K^+ signalling hypothesis mainly utilises the astrocyte, positioned to enable the communication between the neurons and the local perfusing blood vessels. The astrocyte and the endothelial cells (ECs) surrounding the perfusing vessel lumen exhibit a striking similarity in ion channel expression and thus can enable control of the smooth muscle cell (SMC) from both the neuronal and blood vessel components [12]. Whenever there is neuronal activation K^+ ions are released into the extracellular space (ECS) and synaptic cleft (SC). The astrocyte is depolarised by taking up K^+ released by the neuron and releases it into the perivascular space (PVS) via the endfeet through the BK channels [7]. This increase in ECS K^+ concentration ($3 - 10$ mM) near the arteriole hyperpolarises the SMC through the inward rectifying K^+ (KIR) channel, effectively closing the voltage-gated Ca^{2+} channel, reducing smooth muscle cytosolic Ca^{2+} and thereby causing dilation. Higher K^+ concentrations in the PVS cause contraction due to the reverse flux of the KIR channel [6].

Amidst the difficulty in monitoring and measuring the rapid changes in metabolic demands in the highly heterogeneous brain, speculative estimates of the relative demands of the cerebral processes that require energy were given based on different experimental data by Ames [1]. As per the estimate, the vegetative processes that maintain the homeostasis including protein synthesis accounted for $10 - 15\%$ of the total energy consumption. The costliest function seems to be in restoring the ionic gradients during neural activation. The sodium potassium (Na^+/K^+) exchange pump is estimated to consume $40 - 50\%$, while the

Ca^{2+} influx from organelles and extracellular fluid consumes 3 – 7%. The processing of neurotransmitters such as uptake or synthesis consumes 10 – 20%, while the intracellular signalling systems which includes activation and inactivation of proteins consumes 20 – 30%. The rest of the energy is estimated to be consumed by the axonal and dendritic transport in both directions.

Previous work [?] has provided the construction of an experimentally validated numerical (*in silico*) model based on experimental data to simulate the fMRI BOLD signal associated with NVC along with the associated metabolic and blood volume responses. An existing neuron model [14, 15] has been extended to include an additional transient sodium (Na^+) ion channel (NaT) expressed in the neuron, and integrated into a complex NVC model [5, 4, 9]. This present model is based on the hypothesis that the K^+ signalling mechanism of NVC is the primary contributor to the vascular response and the Na^+/K^+ exchange pump in the neuron is the primary consumer of oxygen during neural activation. The model contains 160 parameters, most of which come from non-human experiments.

Such a complex model constructed with a high-dimensional parameter space is not easily amenable to sensitivity analyses considering the significant computing resource required. Indeed no formal theory exists which allows direct mathematical investigation of the variability of the large dimensional parameter vector and the resulting output. From a purely physiological perspective an understanding of the dominant cellular mechanisms resulting in cerebral tissue perfusion after neuronal stimulation would be of particular interest.

We have used the cerebral blood flow (CBF) change from the experimental data [20] taken from the rat barrel cortex.

2 Methodology

some text here

2.1 Simulated Data

We use a square pulse of 10 seconds duration for stimulation such that the resulting output (after a substantial number of realizations) can be analysed in a formal manner. We assume that stimulation occurs for $t_1 \leq t \leq t_2$.

2.2 QoIs

We analyse 3 quantities of interest (QoIs) with respect to the 10 second square stimulation pulse. They are defined as follows.

1. ECS potassium has a distinct effect on the flux into the Neuron. Hence we look at the average.

$$\frac{1}{t_2 - t_1} \int_{t_1}^{t_2} [K^+]_{ECS}(s) ds \quad (2.1)$$

2. As a representation of the volumetric flow rate in the cerebral tissue

$$\frac{1}{t_2 - t_1} \int_{t_1}^{t_2} \left(\frac{R(s)}{R_0} \right)^4 ds \quad (2.2)$$

3. the combined concentration of the actin myosin complex, both phosphorylated and unphosphorylated, determines the effect stress due to the contraction for the smooth muscle cell.

$$[AM + AM_p]_{min} \tag{2.3}$$

2.3 Experimental Data

We repeat analysis of the 3 QoI's listed above

3 Results

This section contains numerical results for 6 QoI's, 3 using a square pulse stimulus and 3 using the experimental data stimulus. The section is organized into 3 subsection where each subsection contains 2 sub-subsections with the results using the square pulse stimulus and experimental data stimulus. For each case we report results using a linear regression to screen out unimportant variables followed by a Polynomial Chaos expansion (PCE) fit on the subset of variables which linear regression deemed as important. The normalized absolute value of linear regression coefficients and the PCE's Sobol' indices are given.

Things we'll need to add:

- Discussion of ODE solver
- Discussion of how the parameter distribution is determined
- Discussion of how the solution regimes were sorted

- Discussion of which parameters determine the solution regime
- Discussion of the surrogate models and Sobol' indices

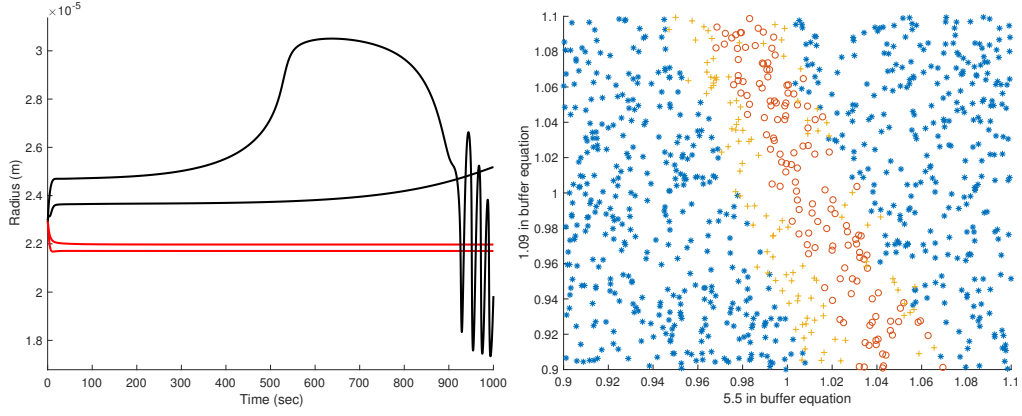


Figure 1: Left: examples of stable (red) and unstable (black) steady state solutions. Right: samples of the buffer parameters using uniform independent sampling. A blue \cdot indicates the sample yielded a premature termination of the solver, a yellow $+$ indicates the sample yielded an unstable steady state, a red \circ indicates the sample yielded a stable steady state.

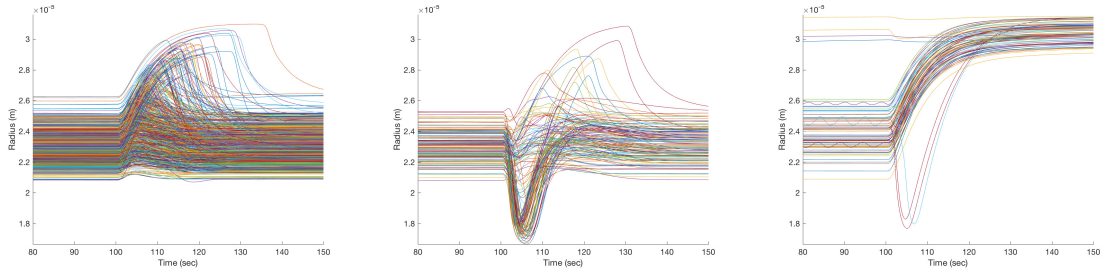


Figure 2: Radii corresponding to samples (using the rectangular pulse stimulus). Left: curves an an increase in response to the stimulus; center: curves with a decrease in response to the stimulus; right: curves which settle in a different steady state.

3.1 QoI (1) (K_{ECS} Mean)

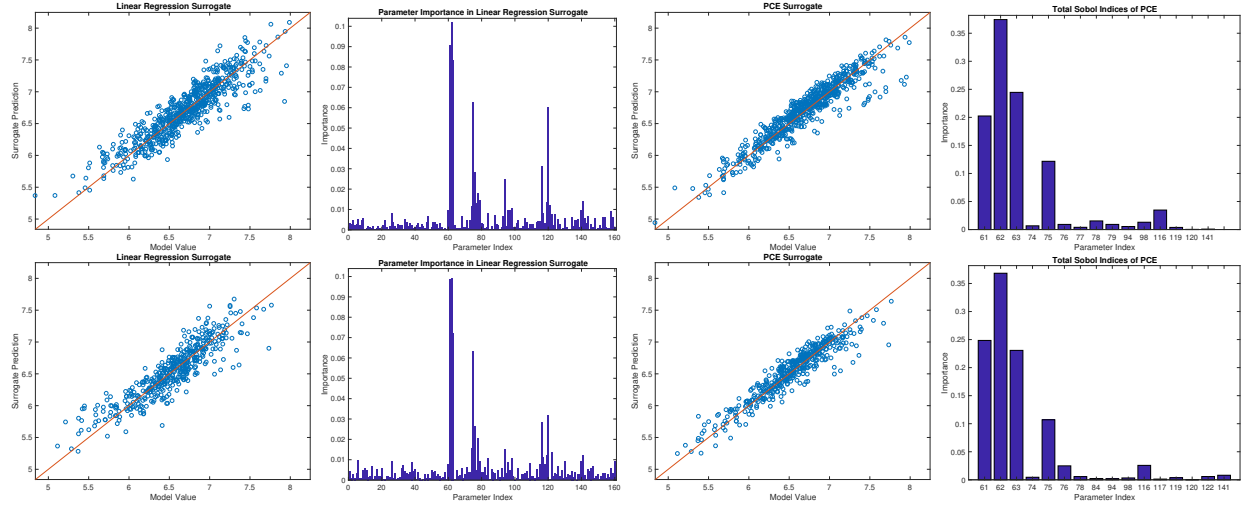


Figure 3: Top row: results with a rectangular pulse stimulus; bottom row: results with experimental data stimulus. From left to right, linear regression predictions, linear regression variable importance, PCE predictions, total Sobol' indices for PCE.

Index	Identification	Total Sobol' Index (RP)	Total Sobol' Index (ES)
62	0.143 in m4alpha and m4 beta	0.3744	0.3683
63	5.67 in m4alpha and m4 beta	0.2446	0.2307
61	gKleak_d in Neuron	0.2025	0.2485
75	34.9 in m6alpha	0.1217	0.1070
116	dhod in Neuron	0.0348	0.0257

Table 1: K_{ECS} Mean

3.2 QoI (2.2) (volumetric flow rate)

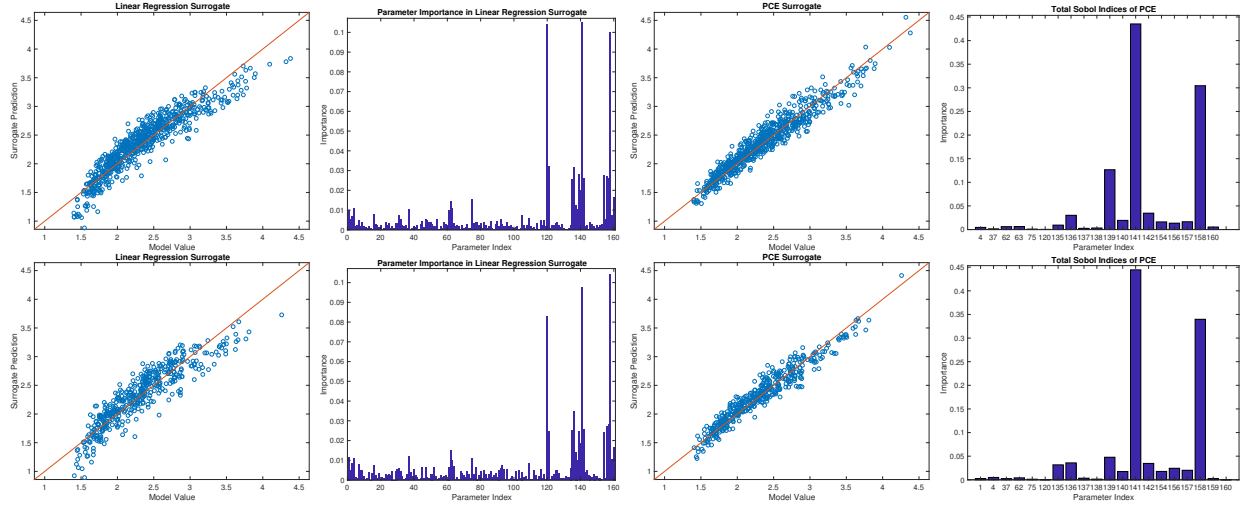


Figure 4: Top row: results with a rectangular pulse stimulus; bottom row: results with experimental data stimulus. From left to right, linear regression predictions, linear regression variable importance, PCE predictions, total Sobol' indices for PCE.

Index	Identification	Total Sobol' Index (RP)	Total Sobol' Index (ES)
141	z_4 in SMCEC	0.4353	0.4445
158	n_cross in WallMechanics	0.3045	0.3398
139	z_2 in SMCEC	0.1267	0.0478
142	z_5 in SMCEC	0.0347	0.0347
136	G_K_i in SMCEC	0.0302	0.0359

Table 2: volumetric flow rate

3.3 QoI (2.3) ($AM + AM_p$ Min)

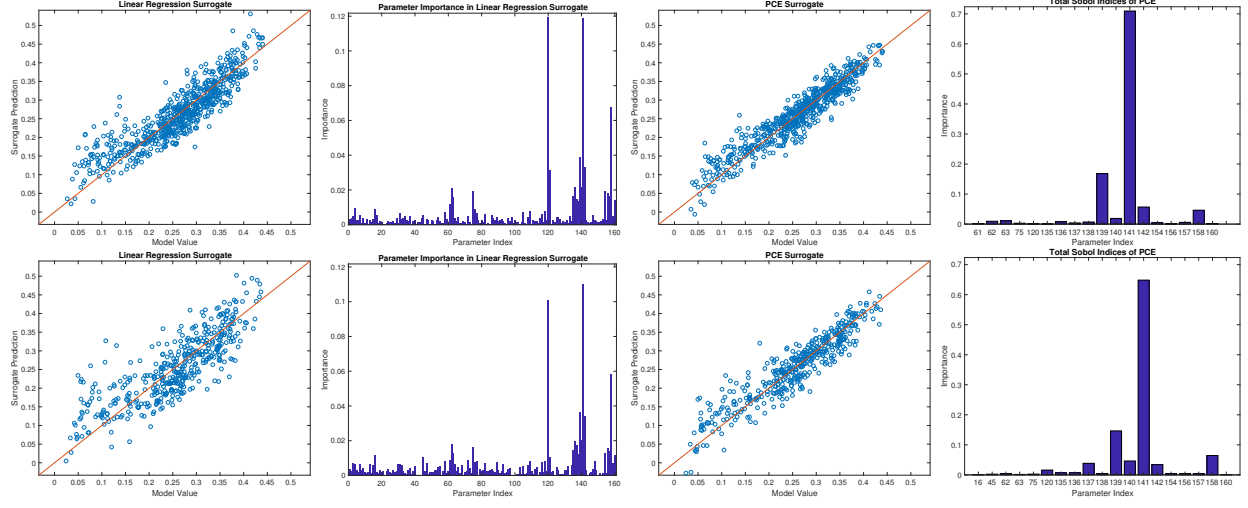


Figure 5: Top row: results with a rectangular pulse stimulus; bottom row: results with experimental data stimulus. From left to right, linear regression predictions, linear regression variable importance, PCE predictions, total Sobol' indices for PCE.

Index	Identification	Total Sobol' Index (RP)	Total Sobol' Index (ES)
141	z_4 in SMCEC	0.7095	0.6485
139	z_2 in SMCEC	0.1681	0.1465
142	z_5 in SMCEC	0.0569	0.0341
158	n_cross in WallMechanics	0.0463	0.0645
140	z_3 in SMCEC	0.0189	0.0463

Table 3: $AM + AM_p$ Min

3.4 AM_p Time Lag

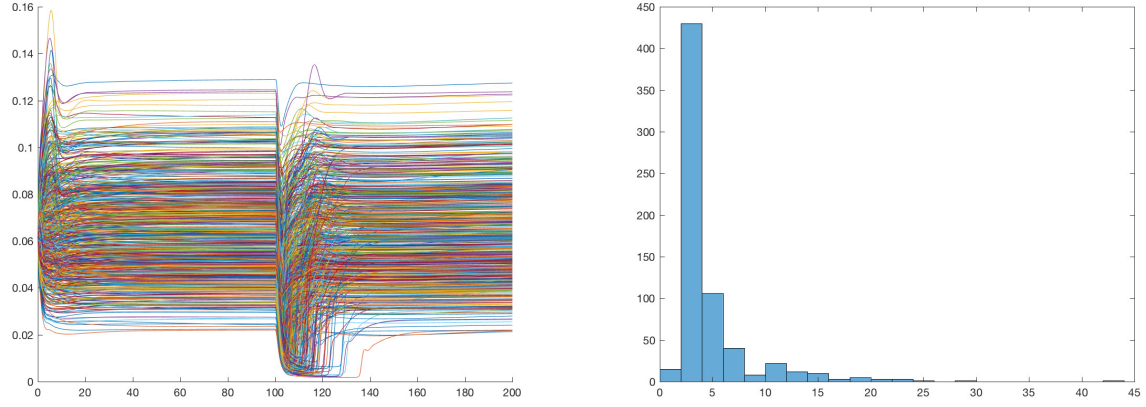


Figure 6: AM_p curves on the left and a histogram of the time lags on the right.

3.5 Radius Time Lag

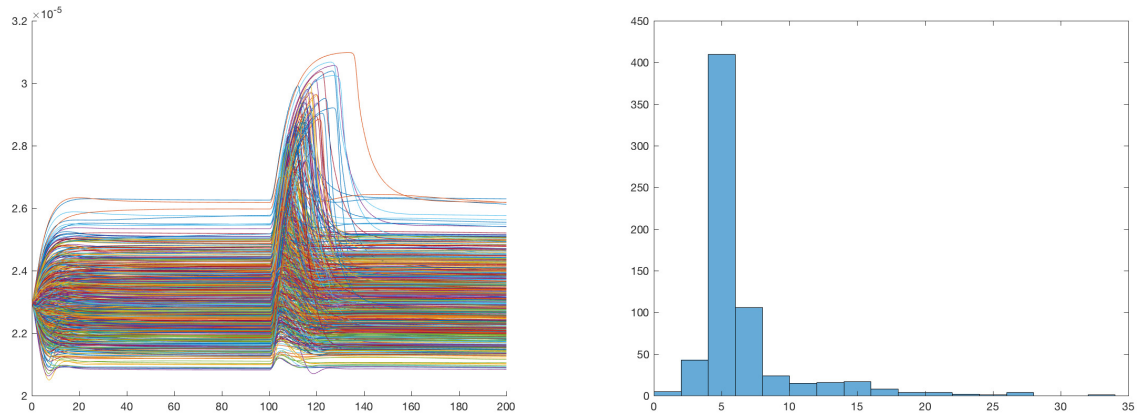


Figure 7: Radius curves on the left and a histogram of the time lags on the right.

4 Discussion

5 Conclusion

References

- [1] **Ames, A. (2000):** CNS energy metabolism as related to function, Brain Research Reviews, Vol. 34 pp. 42–68.
- [2] **Attwell, D.; Buchan, A. M.; Charpak, S.; Lauritzen, M.; MacVicar, B. a. and Newman, E. a. (2010):** Glial and neuronal control of brain blood flow., Nature, Vol. 468, No. 7321 pp. 232–243.
- [3] **Buxton, R. B.; Uluda, K.; Dubowitz, D. J.; Liu, T. T.; Uluda, K.; Dubowitz, D. J. and Liu, T. T. (2004):** Modeling the hemodynamic response to brain activation, NeuroImage, Vol. 23, No. SUPPL. 1 pp. 220–233.
- [4] **Dormanns, K.; Brown, R. G. and David, T. (2016):** The role of nitric oxide in neurovascular coupling, Journal of theoretical biology, Vol. 394 pp. 1–17.
- [5] **Dormanns, K.; van Disseldorp, E. M. J.; Brown, R. G. and David, T. (2015):** Neurovascular coupling and the influence of luminal agonists via the endothelium, Journal of Theoretical Biology, Vol. 364 pp. 49–70.
- [6] **Farr, H. and David, T. (2011):** Models of neurovascular coupling via potassium and EET signalling., Journal of theoretical biology, Vol. 286, No. 1 pp. 13–23.

- [7] **Filosa, J. A.; Blanco, V. M. V. M.; Filosa J.A. Blanco, V. M.; Filosa, J. A. and Blanco, V. M. V. M. (2007):** Neurovascular coupling in the mammalian brain., Experimental physiology, Vol. 92, No. 4 pp. 641–646.
- [8] **Filosa, J. A.; Bonev, A. D.; Straub, S. V.; Meredith, A. L.; Wilkerson, M. K.; Aldrich, R. W. and Nelson, M. T. (2006):** Local potassium signaling couples neuronal activity to vasodilation in the brain, Nature neuroscience, Vol. 9, No. 11 pp. 1397–1403.
- [9] **Kenny, A.; Plank, M. J. and David, T. (2017):** The role of astrocytic calcium and TRPV4 channels in neurovascular coupling, Journal of Computational Neuroscience, Vol. doi pp. 10.1007/s10827-017-0671-7.
- [10] **Leithner, C.; Rojl, G.; Offenhauser, N.; Fächtemeier, M.; Kohl-Bareis, M.; Villringer, A.; Dirnagl, U. and Lindauer, U. (2010):** Pharmacological uncoupling of activation induced increases in CBF and CMRO₂., Journal of cerebral blood flow and metabolism : official journal of the International Society of Cerebral Blood Flow and Metabolism, Vol. 30, No. 2 pp. 311–322.
- [11] **Lindauer, U.; Leithner, C.; Kaasch, H.; Rohrer, B.; Foddiss, M.; Fächtemeier, M.; Offenhauser, N.; Steinbrink, J.; Rojl, G.; Kohl-Bareis, M. and Dirnagl, U. (2010):** Neurovascular coupling in rat brain operates independent of hemoglobin deoxygenation, Journal of Cerebral Blood Flow & Metabolism, Vol. 30, No. 4 pp. 757–768.

- [12] **Longden, T. A.; Hill-eubanks, D. C. and Nelson, M. T. (2015):** Ion channel networks in the control of cerebral blood flow, *Journal of Cerebral Blood Flow & Metabolism*, Vol. 36 pp. 492–512.
- [13] **Makani, S. and Chesler, M. (2010):** Rapid rise of extracellular pH evoked by neural activity is generated by the plasma membrane calcium ATPase., *Journal of neurophysiology*, Vol. 103, No. 2 pp. 667–676.
- [14] **Mathias, E. J.; Plank, M. J. and David, T. (2017):** A model of neurovascular coupling and the BOLD response: PART I, *Computer Methods in Biomechanics and Biomedical Engineering*, Vol. 20, No. 5 pp. 508–518.
- [15] **Mathias, E. J.; Plank, M. J. and David, T. (2017):** A model of neurovascular coupling and the BOLD response: PART II, *Computer Methods in Biomechanics and Biomedical Engineering*, Vol. 20, No. 5 pp. 519–529.
- [16] **Mintun, M. A.; Lundstrom, B. N.; Snyder, A. Z.; Vlassenko, A. G.; Shulman, G. L. and Raichle, M. E. (2001):** Blood flow and oxygen delivery to human brain during functional activity: theoretical modeling and experimental data, *Proc Natl Acad Sci U S A*, Vol. 98, No. 12 pp. 6859–6864.
- [17] **Ogawa, S.; Lee, T. M.; Kay, A. R. and Tank, D. W. (1990):** Brain magnetic resonance imaging with contrast dependent on blood oxygenation., *Proceedings of the National Academy of Sciences of the United States of America*, Vol. 87, No. 24 pp. 9868–9872.

- [18] **Powers, W. J.; Hirsch, I. B. and Cryer, P. E. (1996):** Effect of stepped hypoglycemia on regional cerebral blood flow response to physiological brain activation, *Am J Physiol*, Vol. 270, No. 2 Pt 2 pp. H554—9.
- [19] **Roy, C. S. C. S. and Sherrington, C. S. S. (1890):** On the regulation of the blood-supply of the brain, *The Journal of physiology*, Vol. 11, No. 1-2 p. 85.
- [20] **Zheng, Y.; Pan, Y.; Harris, S.; Billings, S.; Coca, D.; Berwick, J.; Jones, M.; Kennerley, A.; Johnston, D.; Martin, C.; Devonshire, I. M. and Mayhew, J. (2010):** A dynamic model of neurovascular coupling: Implications for blood vessel dilation and constriction, *NeuroImage*, Vol. 52, No. 3 pp. 1135–1147.